Yuan *et al. Nanoscale Research Letters* (2017) 12:574
DOI 10.1186/s11671-017-2330-3

Nanoscale Research Letters

NANO EXPRESS

Conduction Mechanism and Improved Endurance in HfO_2-Based RRAM with Nitridation Treatment

Fang-Yuan Yuan[1], Ning Deng[1,2*], Chih-Cheng Shih[3,4], Yi-Ting Tseng[4], Ting-Chang Chang[4,5*], Kuan-Chang Chang[6], Ming-Hui Wang[3], Wen-Chung Chen[3], Hao-Xuan Zheng[4], Huaqiang Wu[1,2], He Qian[1,2] and Simon M. Sze[7]

Abstract

A nitridation treatment technology with a urea/ammonia complex nitrogen source improved resistive switching property in HfO_2-based resistive random access memory (RRAM). The nitridation treatment produced a high performance and reliable device which results in superior endurance (more than 10^9 cycles) and a self-compliance effect. Thus, the current conduction mechanism changed due to defect passivation by nitrogen atoms in the HfO_2 thin film. At a high resistance state (HRS), it transferred to Schottky emission from Poole-Frenkel in HfO_2-based RRAM. At low resistance state (LRS), the current conduction mechanism was space charge limited current (SCLC) after the nitridation treatment, which suggests that the nitrogen atoms form Hf–N–Ox vacancy clusters (V_o^+) which limit electron movement through the switching layer.

Keywords: HfO_2-based RRAM, Nitridation, Endurance, Space charge limit current

Background

Recently, resistance random access memory (RRAM) composed of an insulating layer sandwiched by two electrodes has been widely studied as a promising candidate for next-generation nonvolatile memory due to its superior properties such as simple structure, low power consumption, high-speed operation (< 300 ps), and nondestructive readout [1–9]. Although most RRAM devices have many properties superior to nonvolatile memory, the high operation current of RRAM and performance degradation are major issues in nonvolatile memory in terms of the application of portable electronic products.

The Pt/HfO_2/TiN structure can supply a conduction path which induces a resistive switching behavior [10–19]. However, the defects of amorphous HfO_2 will increase the number of leakage paths, leading to power consumption and joule heating degradation. In this work, the resistive switching layer of HfO_2 was treated by a solution with a urea/ammonia complex nitrogen source as the nitridation treatment to enhance its electrical switching properties.

Methods

The patterned TiN/Ti/SiO_2/Si substrate was fabricated with a standard deposition and etching process, after which via holes can be formed (inset of Fig. 1a). Then, a 23-nm-thick HfO_2 thin film was deposited into via holes on the substrate by RF magnetron sputtering using a pure HfO_2 target. The sputtering power was fixed at RF power of 150 W and was carried out in argon ambient (Ar = 30 sccm) with a working pressure of 4 mtorr at room temperature. The HfO_2/TiN semi-finished device was put into the reactive chamber and immersed into the solution with a urea/ammonia complex nitrogen source for nitridation treatment. During the nitridation treatment, the solution was heated to 160 °C in the system's stainless steel chamber for 30 min. Then, the 110-nm-thick Pt top electrode was deposited by DC magnetron sputtering on the HfO_2 thin film to form electrical devices with Pt/HfO_2/TiN sandwich structures. Finally, all of the electric characteristics were measured

---

* Correspondence: ningdeng@tsinghua.edu.cn; tcchang3708@gmail.com
[1] Institute of Microelectronics, Tsinghua University, Beijing 100084, China
[4] Department of Physics, National Sun Yat-Sen University, Kaohsiung 80424, Taiwan
Full list of author information is available at the end of the article

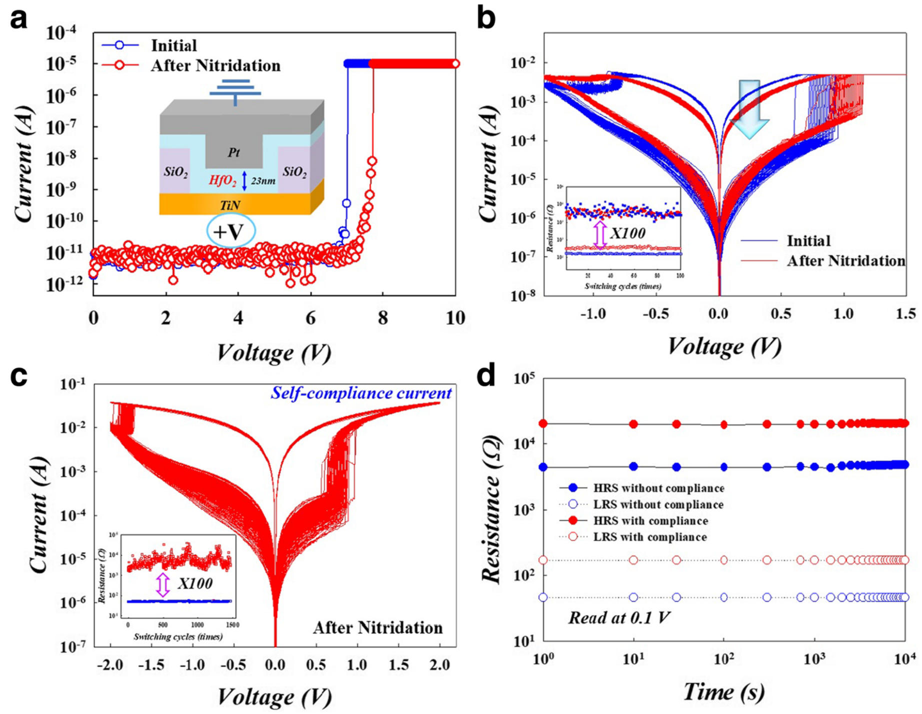

Fig. 1 **a** The forming current curves of HfO_2-based RRAM devices. **b** Comparison of DC sweep cycles at a 5 mA compliance current between initial and after nitridation treatment of HfO_2-based RRAM. **c** DC sweep cycles without external current compliance of the HfO_2 device after nitridation treatment. **d** Retention time of the HfO_2-based RRAM devices at 85 °C with and without compliance current after nitridation treatment

by the Agilent B1500 semiconductor parameter analyzer. The DC and pulse sweeping bias were applied to the bottom electrode (TiN) while the top electrode (Pt) was grounded during the electrical measurements. In addition, Fourier-transform infrared spectroscopy (FTIR) was measured by a Bruker VERTEX 70v spectrometer in the middle infrared region.

Results and Discussion

An electroforming process is required to activate all of the RRAM devices using a DC bias with a compliance current of 10 μA, as shown in Fig. 1a. After the forming process, the electrical current-voltage (I-V) properties of the HfO_2-based RRAM were compared at initial and after the nitridation treatment. At LRS, the current was obviously reduced compared to that of untreated HfO_2 thin film, as shown in Fig. 1b. The current reduction can be attributed to the defects passivated by the NH_3 molecule in the treatment solution. We found that HRS distribution is much more stable after the nitridation treatment, as in the inset of Fig. 1b. The resistance states are extracted with a reading voltage of 0.1 V during the 100 sweep cycles with DC operation (inset of Fig. 1b). The resistance on/off ratio was slightly reduced after the nitridation treatment. Interestingly, a self-compliance resistive switching property was observed in these HfO_2-based RRAM devices after the treatment, as shown in Fig. 1c. After more than 10^3 sweep cycles, a repeatable self-protective characteristic of the device without hard breakdown was observed. The retention time was evaluated at 85 °C and remained stable even after 10^4 s both in HRS and LRS.

To further evaluate device performance, the endurance tests of HfO_2-based RRAM were performed for initial and after the nitridation treatment, as shown in Fig. 2. In the untreated device after 10^6 sweeping cycles, the HRS/LRS ratio significantly degrades from 100:1 to 5:1, as shown in Fig. 2a. After the nitridation treatment, however, even after more than 10^9 sweep cycles, the device exhibited a stable HRS/LRS ratio, as in Fig. 2b. These results indicate that the nitridation process enhanced HfO_2-based RRAM to perform with superior switching features and reliability. To further investigate these results, FTIR analysis was used to observe the chemical alterations of the HfO_2 thin film, as shown in Fig. 3. A sharp peak at 1589 and 1311 cm^{-1} appeared after the nitridation treatment, corresponding to the symmetrical and asymmetrical stretching vibration peak of an N–O bond [20]. Further, the peak intensity of N–H bonds at 1471 cm^{-1} [21] increased due to the nitridation process by urea/ammonia complex nitrogen source (inset of Fig. 3). Therefore, we can infer the formation of nitrogen-containing compounds after the nitridation treatment.

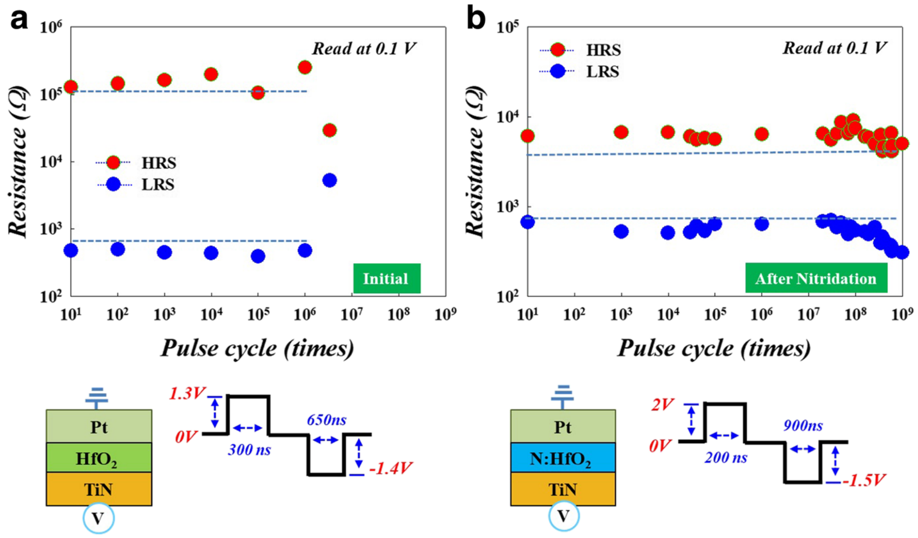

Fig. 2 Comparison of endurance times in HfO_2-based RRAM: **a** initial and **b** after nitridation treatment. The bottom diagrams are the corresponding device structures and endurance pulse conditions

In order to clarify the resistive switching mechanism, we analyzed the current conduction mechanism of the HfO_2 thin film with and without the nitridation treatment, shown in Fig. 4a and d. For the untreated HfO_2 thin film, the electrons were transferred through the defects, such that the current conduction mechanism was dominated by Poole-Frenkel conduction according to the linear relationship between ln(I/V) and the square root of the applied voltage ($V^{1/2}$) on HRS, as shown in Fig. 4b [22].

In contrast, HfO_2-based RRAM exhibited the Schottky emission mechanism according to the linear relationship between ln(I/T^2) and the square root of the applied voltage ($V^{1/2}$) of HRS, as shown in Fig. 4c [23, 24]. This is due to the decrease in defects and dangling bonds, as bonds become passivated by nitrogen atoms after the nitridation treatment. In addition, we also analyzed the current conduction mechanism with and without treatment at LRS in HfO_2-based RRAM. On LRS, the carrier transport mechanism of the untreated HfO_2-based RRAM was dominated by ohmic conduction, where current decreases with increasing temperature, as shown in Fig. 4e. After nitridation treatment, the current conduction mechanism transfers to space charge limited current (SCLC) with a slope of 1.52. The I-V curve is not relative to temperature, with a linear relationship between ln(I) and the square of the applied voltage V^2 on LRS, as shown in Fig. 4f [25].

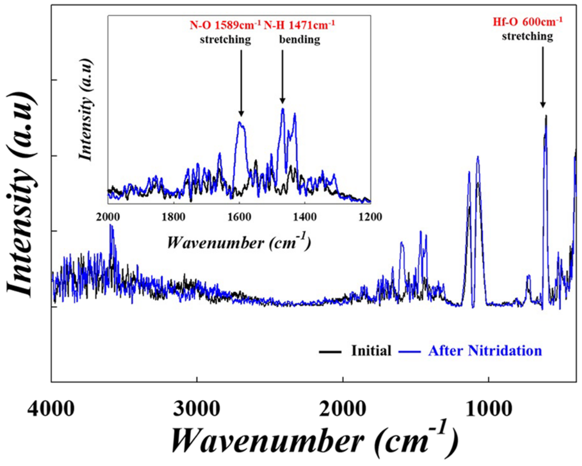

Fig. 3 The comparison of FTIR spectra of HfO_2 thin films between initial and after nitridation treatment

We proposed a model to explain the characteristics of the current conduction mechanism, and it is shown as Fig. 5. Thus, there are two offsetting dipoles associated with N and O atoms and a Hf atom (i.e., the sequence O–Hf–O is replaced by O–Hf–N–O) after doping N atoms into HfO_2 thin film. Because nitrogen electron negativity is lower than oxygen, the dipole of Hf–N bond is lower than the Hf–O bond, which creates a lower dielectric constant region. When a positive bias is applied during the SET process, a series of Hf–N–Ox vacancies are formed due to their lower dielectric constant, then forming vacancy clusters (Vo^+). The conductive path typically forms along with the Hf–N–Ox vacancy clusters (Vo^+) as nitrogen atoms capture oxygen ions around the clusters, as shown in Fig. 5b. The presence of these insulating Hf–N–Ox vacancy clusters (Vo^+) results in current reduction and the self-compliance effect found in HfO_2-based RRAM.

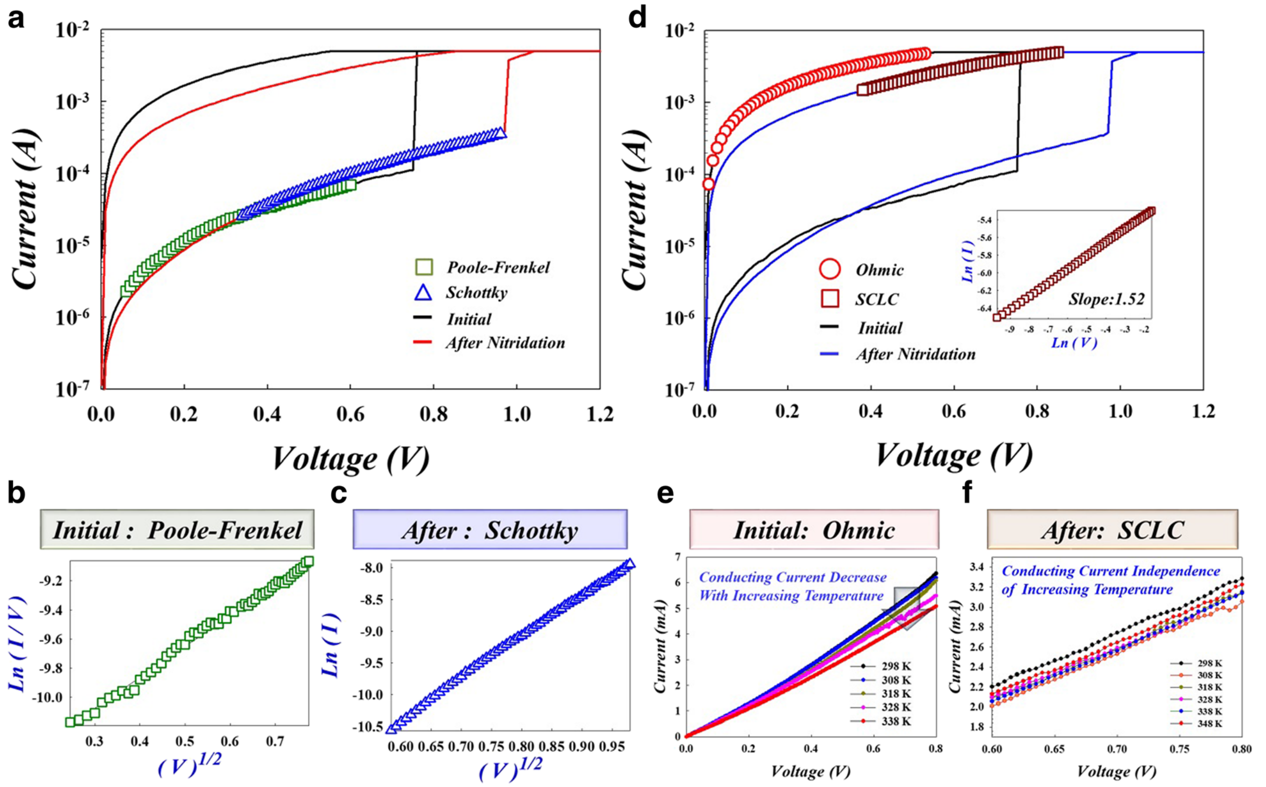

Fig. 4 **a** Analysis current conduction mechanism of HRS from I-V curves in HfO_2-based RRAM between initial and after nitridation treatment. **b** The Poole-Frenkel current conduction mechanism of HRS in HfO_2-based RRAM. **c** The Schottky emission current conduction mechanism of HRS in HfO_2-based RRAM after the nitridation treatment. **d** Analysis current conduction mechanism of LRS which transforms to SCLC from ohmic conduction after nitridation treatment in HfO_2-based RRAM; the inset figure shows the SCLC current fitting result. **e** The Ohmic conduction mechanism of LRS in HfO_2-based RRAM which is characteristic in current negative correlation with temperature. **f** The SCLC mechanism of LRS in HfO_2-based RRAM that is independent on temperature after the nitridation treatment

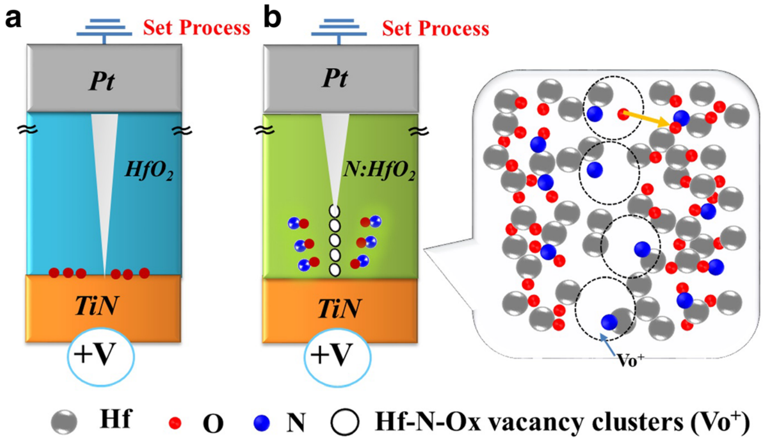

Fig. 5 A schematic of the migration of oxygen ions through the set process in HfO_2-based RRAM for **a** initial and **b** after nitridation treatment, which forms Hf–N–Ox vacancy clusters (V_o^+)

Conclusions

In summary, a self-compliance resistive switching property was observed in a Pt/HfO_2/TiN RRAM device after the nitridation treatment. Endurance times reached 10^9 cycles and a retention time of more than 10^4 s was achieved at 85 °C. Due to the smaller electron negativity of the nitrogen atom when compared to the oxygen atom, the dipole of the Hf–N bond is smaller than that of the Hf–O bond, which creates a lower dielectric constant region. During the SET process, the Hf–N–Ox vacancy clusters (Vo^+) form the conductive path. The insulating Hf–N–Ox vacancy clusters (Vo^+) protect the device from hard breakdown and perform a self-compliance property.

Abbreviations

FTIR: Fourier-transform infrared spectroscopy; HRS: High resistance state; LRS: Low resistance state; RRAM: Resistive random access memory; SCLC: Space charge limited current

Acknowledgments

This work was performed at National Science Council Core Facilities Laboratory for Nano-Science and Nano-Technology in Kaohsiung-Pingtung area and supported by the Ministry of Science and Technology of the Republic of China under Contract No. MOST-106-2112-M-110-008-MY3 and MOST-106-2119-M-110-003.

Availability of data and materials

All data are fully available without restriction.

Authors' contributions

FYY, YTT, and WCC carried out the sample preparation and the measurements. CCS, MHW, and HXZ participated in the discussion. ND, TCC, KCC, HW, HQ, and SMS supervised the project. All the authors have read and approved the final manuscript.

Authors' information

Fang-Yuan Yuan is a doctor of the Institute of Microelectronics, Beijing, Tsinghua University. Ning Deng and Huaqiang Wu are professors of the Institute of Microelectronics, Beijing, Tsinghua University and Tsinghua National Laboratory for Information Science and Technology (TNList). He Qian is a professor of the Institute of Microelectronics, Beijing, Tsinghua University and head of Tsinghua National Laboratory for Information Science and Technology (TNList). Chih-Cheng Shih and Wen-Chung Chen are doctors of the Department of Materials and Optoelectronic Science, Kaohsiung, National Sun Yat-Sen University. Yi-Ting Tseng is a doctor of the Department of Physics, Kaohsiung, National Sun Yat-Sen University. Ting-Chang Chang is a professor of the Department of Physics, Kaohsiung, National Sun Yat-Sen University and Advanced Optoelectronics Technology Center, Taiwan, National Cheng Kung University. Kuan-Chang Chang is an assistant professor of the School of Electronic and Computer Engineering, Shenzhen, Peking University. Simon M. Sze is professor of the Department of Electronics Engineering, Hsinchu, National Chiao Tung University.

Ethics approval and consent to participate

Not applicable.

Consent for publication

Not applicable.

Competing interests

The authors declare that they have no competing interests.

Publisher's Note

Author details

[1]Institute of Microelectronics, Tsinghua University, Beijing 100084, China. [2]Tsinghua National Laboratory for Information Science and Technology (TNList), Beijing 100084, China. [3]Department of Materials and Optoelectronic Science, National Sun Yat-Sen University, Kaohsiung 80424, Taiwan. [4]Department of Physics, National Sun Yat-Sen University, Kaohsiung 80424, Taiwan. [5]Advanced Optoelectronics Technology Center, National Cheng Kung University, Tainan 70101, Taiwan. [6]School of Electronic and Computer Engineering, Peking University, Shenzhen 518055, China. [7]Department of Electronics Engineering, National Chiao Tung University, Hsinchu 300, Taiwan.

Received: 26 May 2017 Accepted: 26 September 2017

References

1. Chang TC, Jian FY, Chen SC, Tsai YT (2011) Developments in nanocrystal memory. Mater Today 14:608–615.
2. Chang TC, Chang KC, Tsai TM, Chu TJ, Sze SM (2016) Resistance random access memory Mater Today 19:254–264.
3. Li YT, Long SB, Zhang MH, Liu Q, Shao LB, Zhang S, Wang Y, Zuo QY, Liu S, Liu M (2010) Resistive switching properties of structure for low-voltage nonvolatile memory applications. IEEE Electron Device Lett 31:117–119.
4. Yang FM, Chang TC, Liu PT, Yeh PH, Yu YC, Lin JY, Sze SM, Lou JC (2007) Memory characteristics of Co nanocrystal memory device with HfO2 as blocking oxide. Appl Phys Lett 90:132102.
5. Son JY, Shin YH (2008) Direct observation of conducting filaments on resistive switching of NiO thin films. Appl Phys Lett 92:833.
6. Syu YE, Chang TC, Tsai TM, Hung YC, Chang KC, Tsai MJ, Kao MJ, Sze SM (2011) Redox reaction switching mechanism in RRAM device with structure. IEEE Electron Device Lett 32:545–547.
7. Shih CC, Chen WJ, Chang KC, Chang TC, Tsai TM, Chu TJ, Tseng YT, Wu CH, Su WC, Chen MC, Huang HC, Wang MH, Chen JH, Zheng JC, Sze SM (2016) Ultra-Low Switching Voltage Induced by Inserting SiO_2 Layer in Indium-Tin-Oxide-Based Resistance Random Access Memory IEEE Electron Device Lett 37:1276–1279.
8. Pan CH, Chang TC, Tsai TM, Chang KC, Chu TJ, Chen PH, Chen MC, Sze SM (2016) Adjustable built-in resistor on oxygen-vacancy-rich electrode-capped resistance random access memory Appl Phys Express 9:104201.
9. Chen PH, Chang KC, Chang TC, Tsai TM, Pan CH, Chu TJ, Chen MC, Huang HC, Lo I, Zheng JC (2016) Bulk Oxygen-Ion Storage in Indium-Tin-Oxide Electrode for Improved Performance of HfO_2-Based Resistive Random Access Memory IEEE Electron Device Lett 37:280-283.
10. Han C, Liu Y, He H (2013) Heterogeneous photochemical aging of soot by NO_2 under simulated sunlight. Atmos Environ 64:270–276.
11. Pan CH, Chang TC, Tsai TM, Chang KC, Chu TJ, Lin WY, Chen MC, Sze SM (2016) Confirmation of filament dissolution behavior by analyzing electrical field effect during reset process in oxide-based RRAM Appl Phys Lett 109: 133503.
12. Zhang W, Hu Y, Chang TC, Tsai TM, Chang KC, Chen HL, Su YT, Zhang R, Hung YC, Syu YE, Chen MC, Zheng JC, Lin HC, Sze SM (2015) Mechanism of Triple Ions Effect in GeSO Resistance Random Access Memory IEEE Electron Device Lett 36:552–554.
13. Lin CY, Chang KC, Chang TC, Tsai TM, Pan CH, Zhang R, Liu KH, Chen HM, Tseng YT, Hung YC, Syu YE, Zheng JC, Wang YL, Zhang W, Sze SM (2015) Effects of Varied Negative Stop Voltages on Current Self-Compliance in Indium Tin Oxide Resistance Random Access Memory IEEE Electron Device Lett 36:564–566.
14. Chang KC, Chang TC, Tsai TM, Zhang R, Hung YC, Syu YE, Chang YF, Chen MC, Chu TJ, Chen HL, Pan CH, Shih CC, Zheng JC, Sze SM (2015) Physical and chemical mechanisms in oxide-based resistance random access memory Nanoscale Research Lett 10.
15. Ye C, Zhan C, Tsai TM, Chang KC, Chen MC, Chang TC, Deng TF, Wang H (2014) Low-power bipolar resistive switching TiN/HfO2/ITO memory with self-compliance current phenomenon Appl Phys Express 7:034101.
16. Chang KC, Tsai TM, Chang TC, Chen KH, Zhang R, Wang ZY, Chen JH, Young TF, Chen MC, Chu TJ, Huang SY, Syu YE, Bao DH, Sze SM (2014) Dual Ion Effect of the Lithium Silicate Resistance Random Access Memory IEEE Electron Device Lett 35:530–532.
17. Chu TJ, Tsai TM, Chang TC, Chang KC, Zhang R, Chen KH, Chen JH, Young TF, Huang JW, Lou JC, Chen MC, Huang SY, Chen HL, Syu YE, Bao, DH, Sze

SM (2014) Tri-Resistive Switching Behavior of Hydrogen Induced Resistance Random Access Memory IEEE Electron Device Lett 35:217–219.
18. Chen YJ, Chen HL, Young TF, Chang TC, Tsai TM, Chang KC, Zhang R, Chen KH, Lou JC, Chu TJ, Chen JH, Bao DH, Sze SM (2014) Hydrogen induced redox mechanism in amorphous carbon resistive random access memory Nanoscale Research Lett 10:52
19. Su YT, Chang KC, Chang TC, Tsai TM, Zhang R, Lou JC, Chen JH, Young TF, Chen KH, Tseng BH, Shih CC, Yang YL, Chen MC, Chu TJ, Pan CH, Syu YE, Sze SM (2013) Characteristics of hafnium oxide resistance random access memory with different setting compliance current Appl Phys Lett 103:163502.
20. Acton O, Ting G, Ma H, Hutchins D, Wang Y, Purushothaman B, Anthony JE, Jen AKY (2008) Π-σ-phosphonic acid organic monolayer/sol-gel hafnium oxide hybrid dielectrics for low-voltage organic transistors. Adv Mater 20: 3697–3701.
21. Coates J (2000) Interpretation of infrared spectra, a practical approach by John Coates in encyclopedia of analytical chemistry. John Wiley&Sons Ltd., Chichester, pp 10815–10837.
22. Frenkel J (1938) On pre-breakdown phenomena in insulators and electronic semi-conductors. Phys Rev 54:647–648.
23. Das RR, Bhattacharya P, Perez W, Katiyar RS, Bhalla AS (2002) Leakage current characteristics of laser-ablated $SrBi_2Nb_2O_9$ thin films. Appl Phys Lett 81:880.
24. Chu TJ, Tsai TM, Chang TC, Chang KC, Pan CH, Chen KH, Chen JH, Chen HL, Huang HC, Shih CC, Syu YE, Zheng JC, Sze SM (2014) Ultra-high resistive switching mechanism induced by oxygen ion accumulation on nitrogen-doped resistive random access memory. Appl Phys Lett 105:223514.
25. Harada T, Ohkubo I, Tsubouchi K, Kumigashira H, Ohnishi T, Lippmaa M, Matsumoto Y, Koinuma H, Oshima M (2008) Trap-controlled space-charge-limited current mechanism in resistance switching at Al/$Pr_{0.7}Ca_{0.3}MnO_3$ interface. Appl Phys Lett 92:222113.